Supplementary Fig. 1

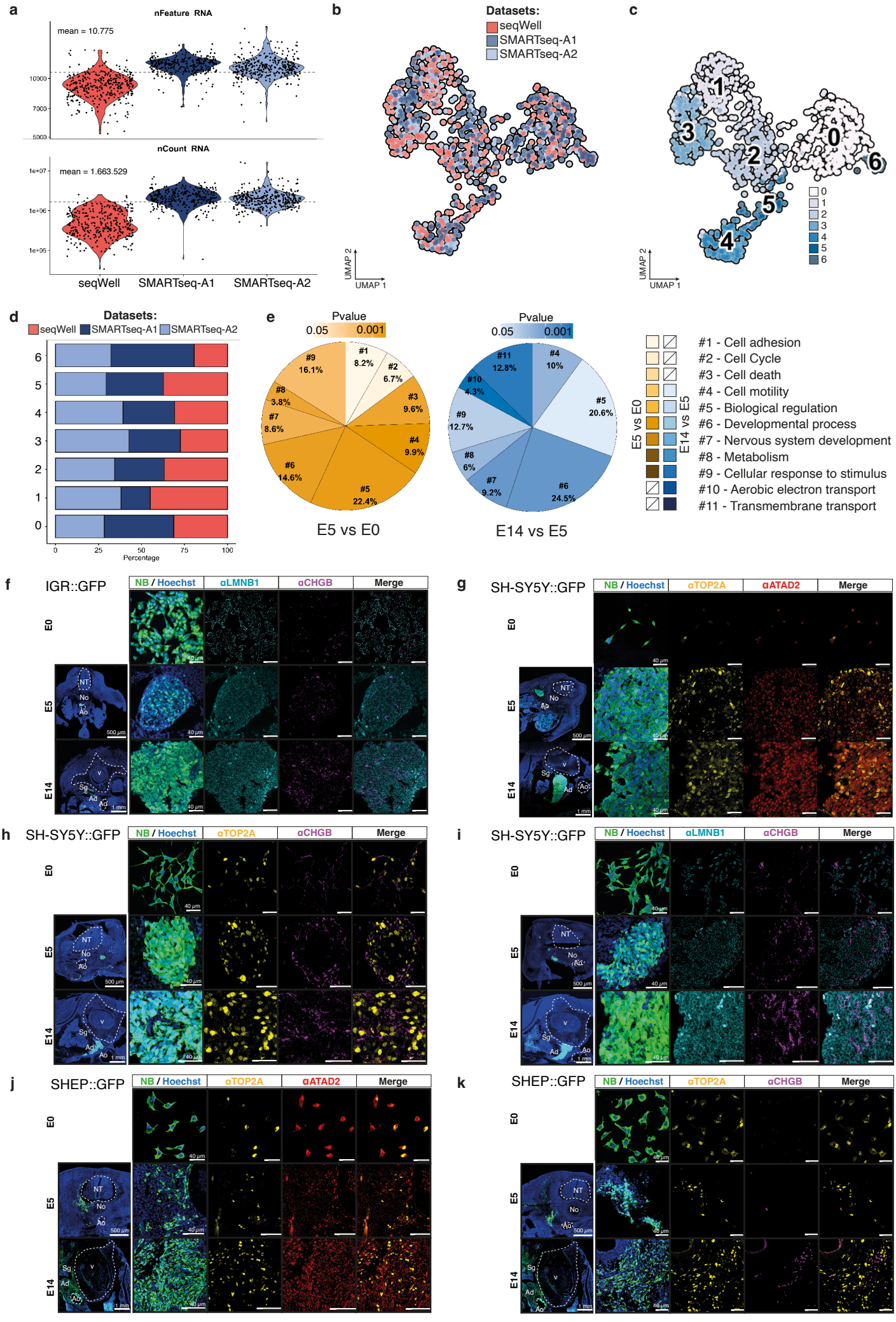

Supplementary Fig. 1 | Transcriptomic evolution of NB cells across disease progression in an avian embryonic microenvironment. a, Violin plots showing quality controls (nFeatures: number of distinct sequenced genes, nCounts: total number of sequenced genes) after sequencing of NB cells harvested at E0, E5 and E14 for each sequencing method (Dataset: SMART-SeqA1, SMART-SeqA2, seqWell). **b,c,** NB cells harvested at E0, E5 and E14 embedded in a UMAP colored by dataset (**b**) or by Louvain clustering (**c**). **d,** Bar plot with fractions of cells in each cluster (c0, c1, c2) sequenced either with SMARTseq-A1/A2 or seqWell. **e**, Pathway enrichment analysis of NB cells over time based on gene differential expression in E5 vs E0 and in E14 vs E5 (two-sided Wilcoxon rank sum test; p-value < 0.05, log fold change > 0.25, min.pct >0.1). Pie plot with pathway categorization (biological processes from gene ontology) of E5 vs E0 (yellow) and E14 vs E5 (blue) are shown (p-value < 0.05). A crossed-out square means that the category is not represented. **f-k,** Representative images of immunofluorescence labeling on IGR-N91::GFP (E5 : N = 10 embryos from 4 independent experiments; E14 : N = 8 embryos from 5 independent experiments) **(f)**, SH-SY5Y::GFP (E5 : N = 11 embryos from 4 independent experiments; E14 : N = 6 embryos from 3 independent experiments) **(g-i)** and SHEP::GFP (E5 : N = 8 embryos from 3 independent experiments; E14 : N = 5 embryos from 2 independent experiments) **(j,k)** cell lines with α-ATAD2 (c0), α-TOP2A (c2), α-LMNB1 (c2,c0) and α-CHGB (c1) antibodies in cell culture and on cryosections of E5 and E14 chick embryos grafted at E2. Scale bars are indicated on the photos. Source data are provided as a source data file.

Adr: Adrenal gland; Ao: Aorta; No: Notochord; NT: Neural Tube; Sg: Sympathetic ganglia; V: Vertebrae.

Supplementary Fig. 2

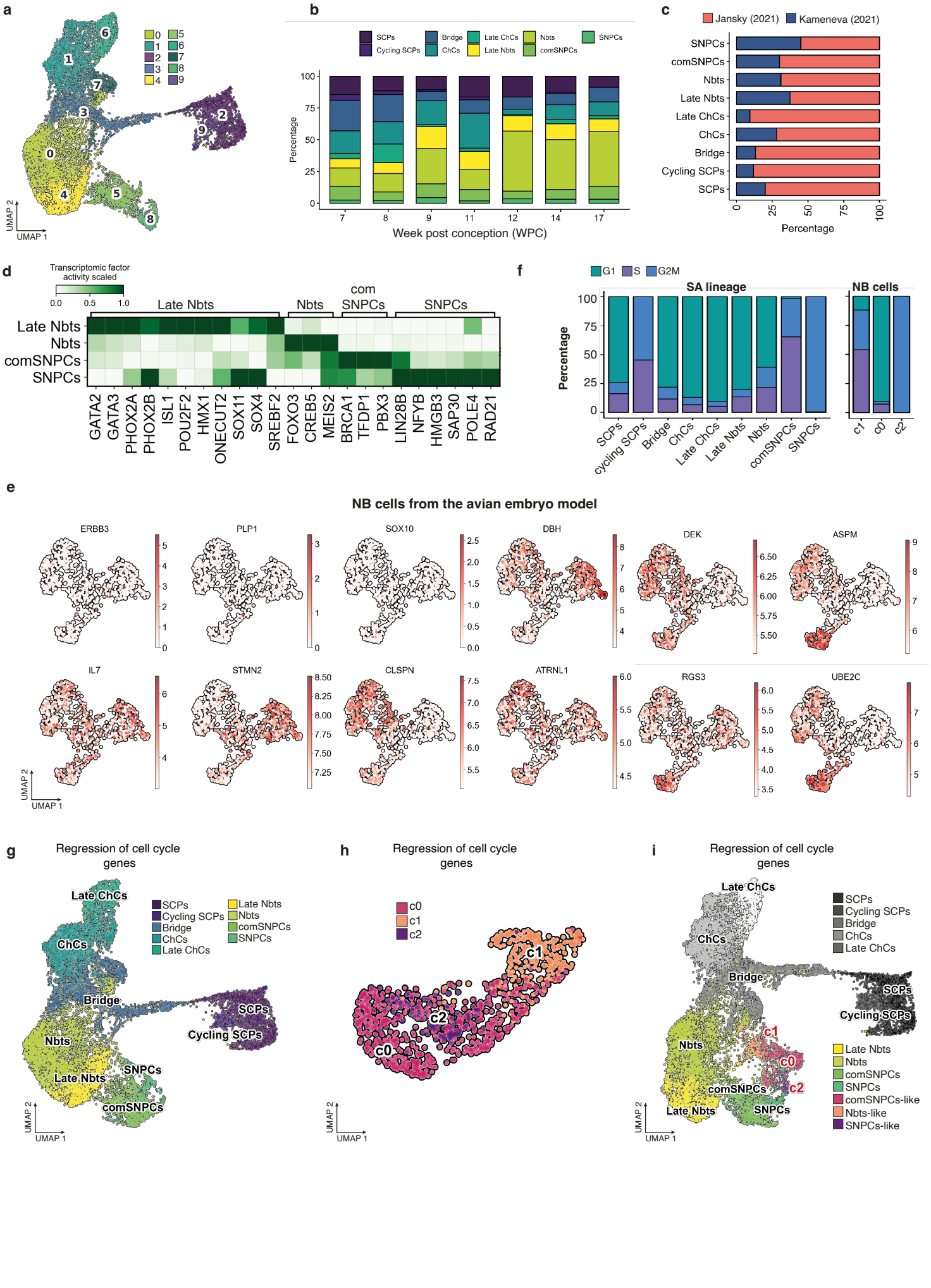

Supplementary Fig. 2 | NB cells replay part of human SNPCs-to-Neuroblasts differentiation program. a, UMAP embedding of 14,443 single cells of the human sympatho-adrenal lineage colored by Louvain clustering**. b,** Bar plot showing the fractions of SA lineage cell states at each developmental time point (WPC: Weeks Post Conception). **c,** Bar plot showing the contribution of each dataset (Jansky et al. [15] and Kameneva et al. [16]) to SA-derived cell states -12,684 single cells from Jansky et al. [15] and 3,704 single cells from Kameneva et al. [16]. **d**, Heatmap of the scaled predicted transcription factor activity for key transcription factors in the SNPCs-to-Neuroblasts differentiation axis. **e,** Expression of key marker genes of the SA lineage in UMAP embedding of NB cells at E14. Color scales indicate log-normalized gene expression. **f,** Bar plot with fractions of cells in each cell cycle phase in the human SA lineage and in NB cells harvested from grafted chick embryos using dataset of murine hematopoietic progenitors as a reference (Nestorowa et al., Blood 2016). **g,h,** UMAP plot of the human SA atlas (**g**) and of NB cells harvested from chick embryos (**h**) colored by transcriptomic state after regression of cell genes**. i**, Unimodal projection UMAP of NB cells -colored by transcriptomic states- mapped onto the human SA lineage atlas after regression of cell cycle genes**.** Source data are provided as a source data file.

Supplementary Fig. 3

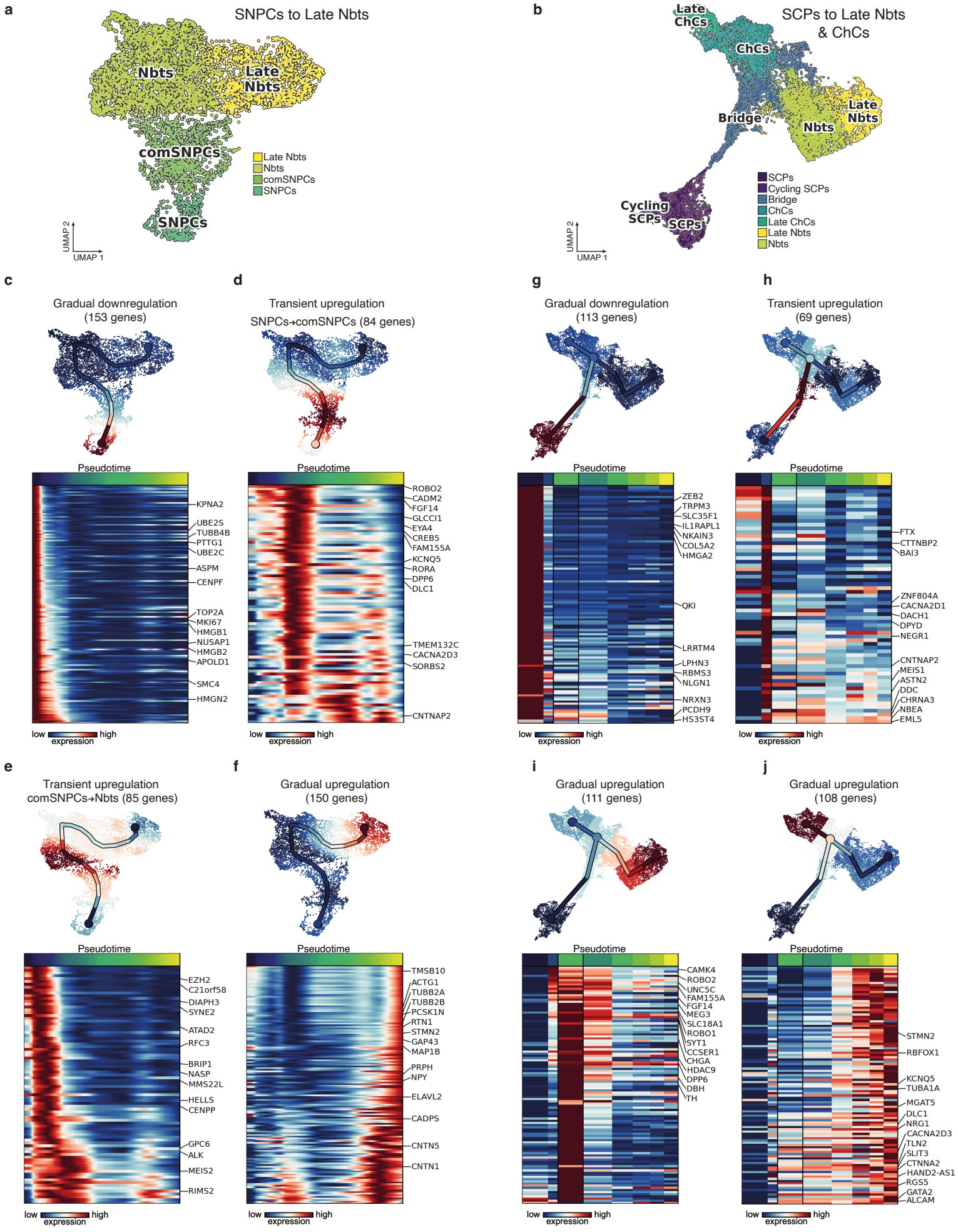

Supplementary Fig. 3 | Human SNPCs and SCPs differentiation programs. a,b Subsetting and re-clustering of SNPCs-to-late neuroblasts (**a**) and SCPs-to-late neuroblasts or chromaffin cells (**b**) differentiation axes in UMAP embeddings. **c-f,** Heatmaps and corresponding sets of genes which expression significantly vary along linear pseudotime of the SNPCs-to-late neuroblasts differentiation trajectory using Moran's I test. **g-j,** Heatmaps and corresponding sets of genes which expression significantly vary along linear pseudotime of the SCPs-to-late neuroblasts or chromaffin cells differentiation trajectory using Moran's I test. Source data are provided as a source data file.

Supplementary Fig. 4

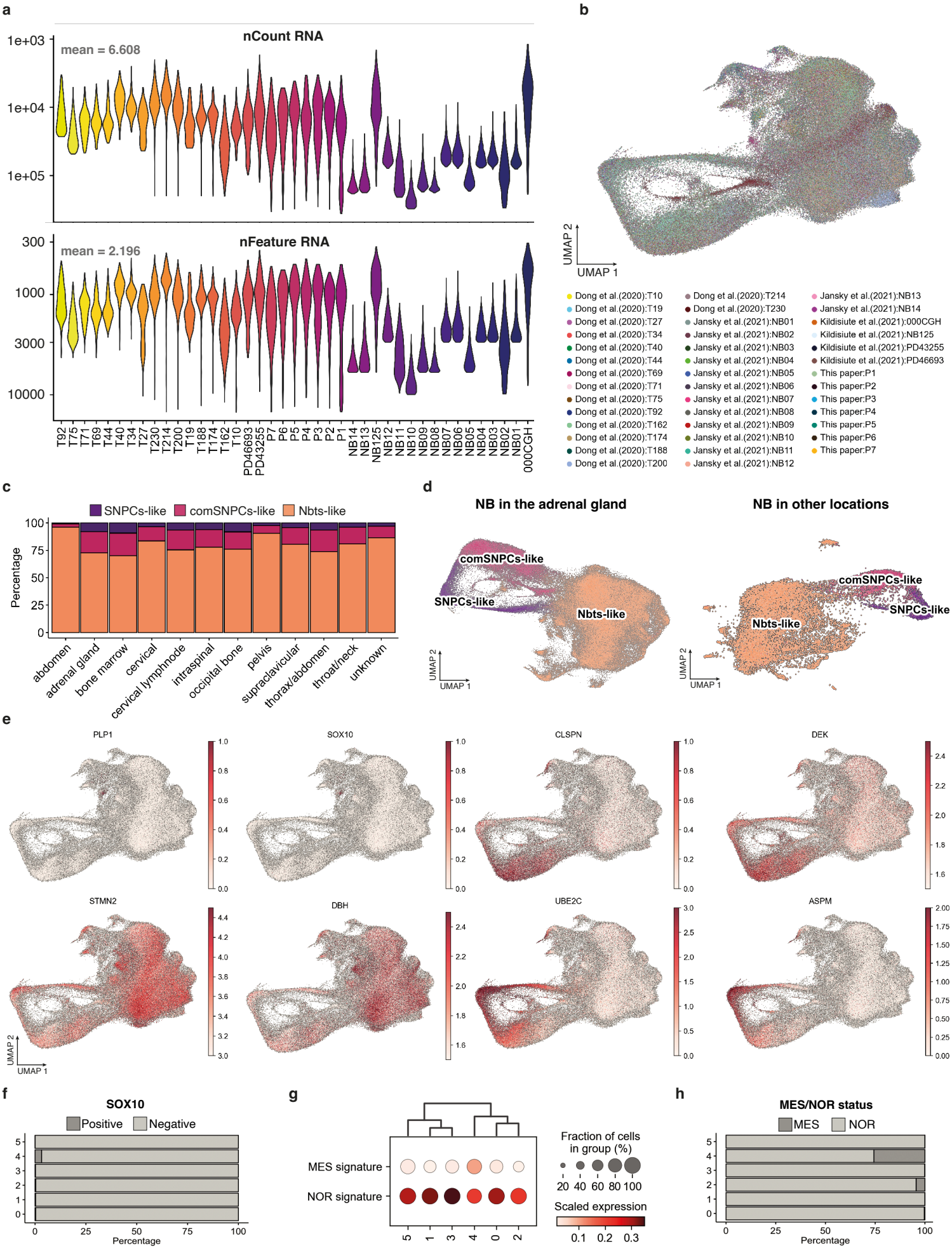

Supplementary Fig. 4 l scRNA-seq analysis of NB patient samples. a, Violin plot showing data quality control of scRNASeq data from NB patient samples. The total number of sequenced genes (top) and the number of distinct sequenced genes (bottom) are shown. **b**, UMAP plot of NB cells from patient samples colored and labeled by patient. **c,** Bar plot of fractions of NB cells assigned to SA-related transcriptomic states (SNPCs-like, comSNPCs-like, Nbts-like) depending on patient tumor anatomical location. **d**, UMAP plot of integrated NB cells colored by SA-related transcriptomic states (SNPCs-like, comSNPCs-like, Nbts-like) either in adrenal tumor samples (left) or in other tumor anatomical locations (right). **e,** Expression of key marker genes of the SA lineage in UMAP embedding of NB patient cells. Color scales indicate log-normalized gene expression. **f**, Bar plot showing fractions of cells expressing SOX10 transcript in each NB patient cell cluster. **g,** Dot plot of adrenergic (NOR) and mesenchymal (MES) gene signature scores from Van Groningen et al. (2017) [11] in transcriptomic clusters of NB patient cells. **h,** Bar plot of fractions of cells in each NB patient cell cluster showing a mesenchymal (MES) or noradrenergic (NOR) state (defined as MES score > NOR score or MES score < NOR score respectively). Source data are provided as a source data file.

Supplementary Fig. 5

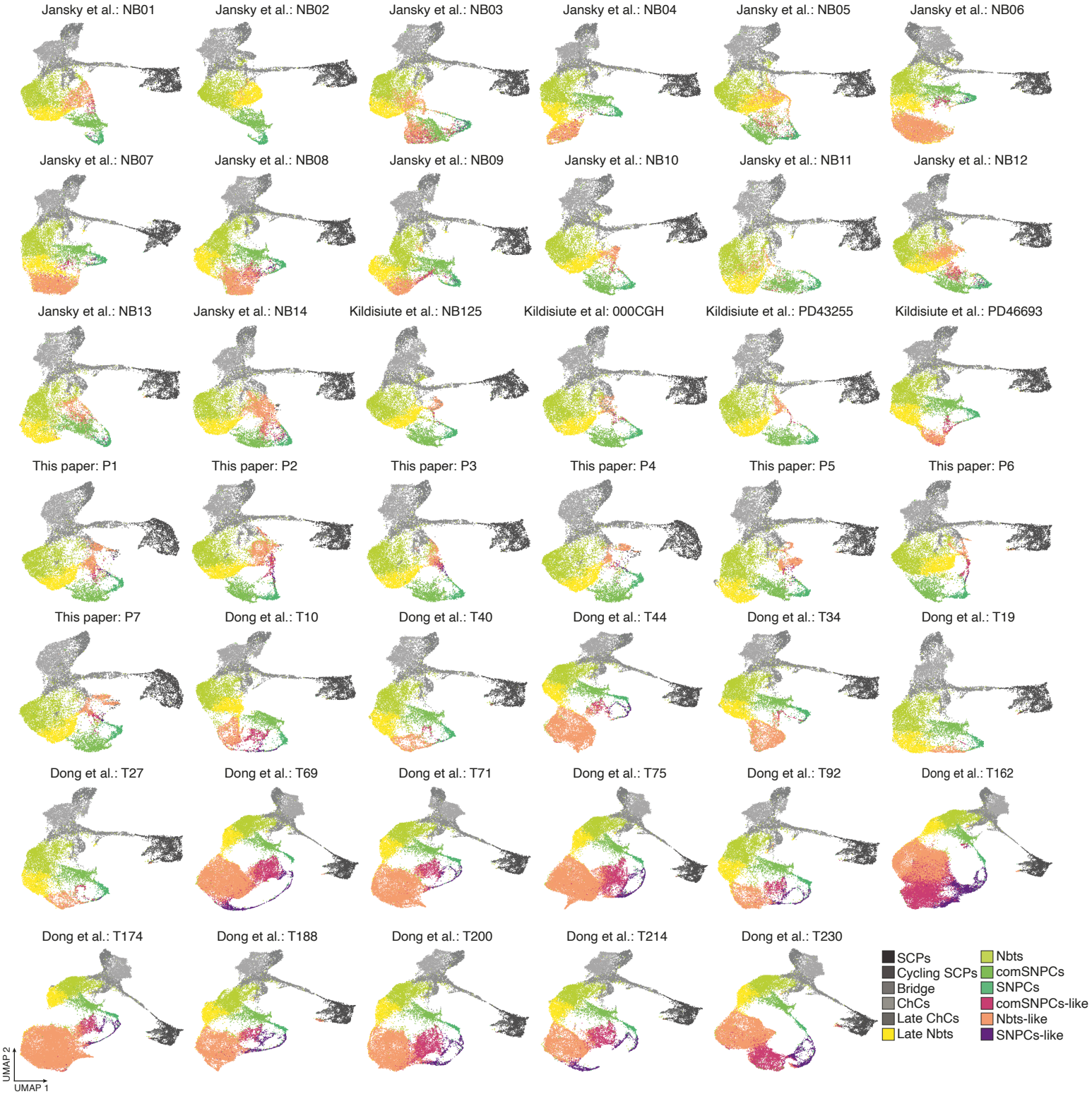

Supplementary Fig. 5 | Projections of NB patient samples onto the human SA lineage. Unimodal UMAP projections of individual NB patient samples (N = 41 samples) onto the human SA lineage UMAP.

Supplementary Fig. 6

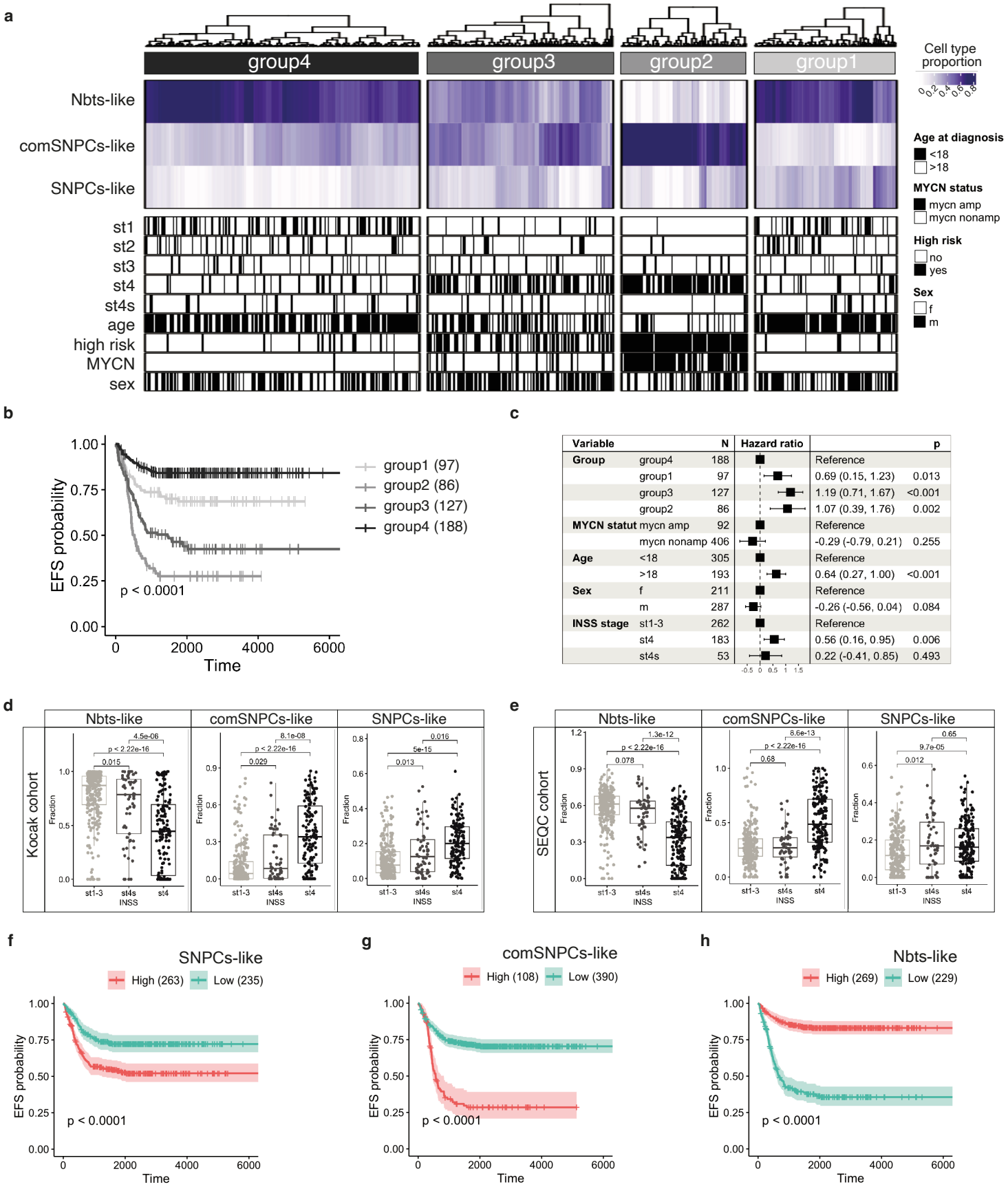

Supplementary Fig. 6 | Analysis of human SNPCs-like/Nbts-like signatures in NB patient cohorts. a, Heatmap with hierarchical clustering of 498 RNA-seq patient samples from SEQC's cohort [25] with associated clinical information based on deconvolution, using patient NB scRNA-seq atlas as a reference to assess proportion of NB transcriptomic states. **b,** Kaplan–Meier analysis of event free survival (EFS) in NB patients of the SEQC cohort according to SA lineage-related hierarchical clustering (group 1 to 4). Log-rank test with Bonferroni adjustment was performed to compare survival curves. **c,** Forest plot of hazard ratio in SEQC cohort depending on SA lineage-related NB profiles (group 1 to 4) from Cox regression EFS analyses in multivariable analyses adjusted for age, sex, MYCN status and INSS classification. Error bars represent the 95% confidence interval of the likelihood test performed on the calculated hazard ratio (two-sided test). **d,e,** Fraction of SNPCs-like, comSNPCs-like and Nbts-like states in NB patient samples according to INSS stages in Kocak (**d**) and SEQC (**e**) cohorts. Statistical significance was determined by two-sided Wilcoxon rank-sum test. In box plots, each point corresponds to a patient sample. The centre line denotes the median value (50th percentile), while the bounds of the box contains the 25th to 75th percentiles of dataset. The whiskers mark the 1.5 times the interquartile rangemark from the upper and lower bounds of the box, and values beyond these upper and lower limits are considered outliers. **f-h**, Kaplan–Meier analysis of EFS in NB patients of SEQC cohort according to the relative proportion of SNPCs-like (**f**), comSNPCs-like (**g**) or Nbts-like states (**h**). Log-rank test was performed. Error bands show the 95% confidence interval.

Supplementary Fig. 7

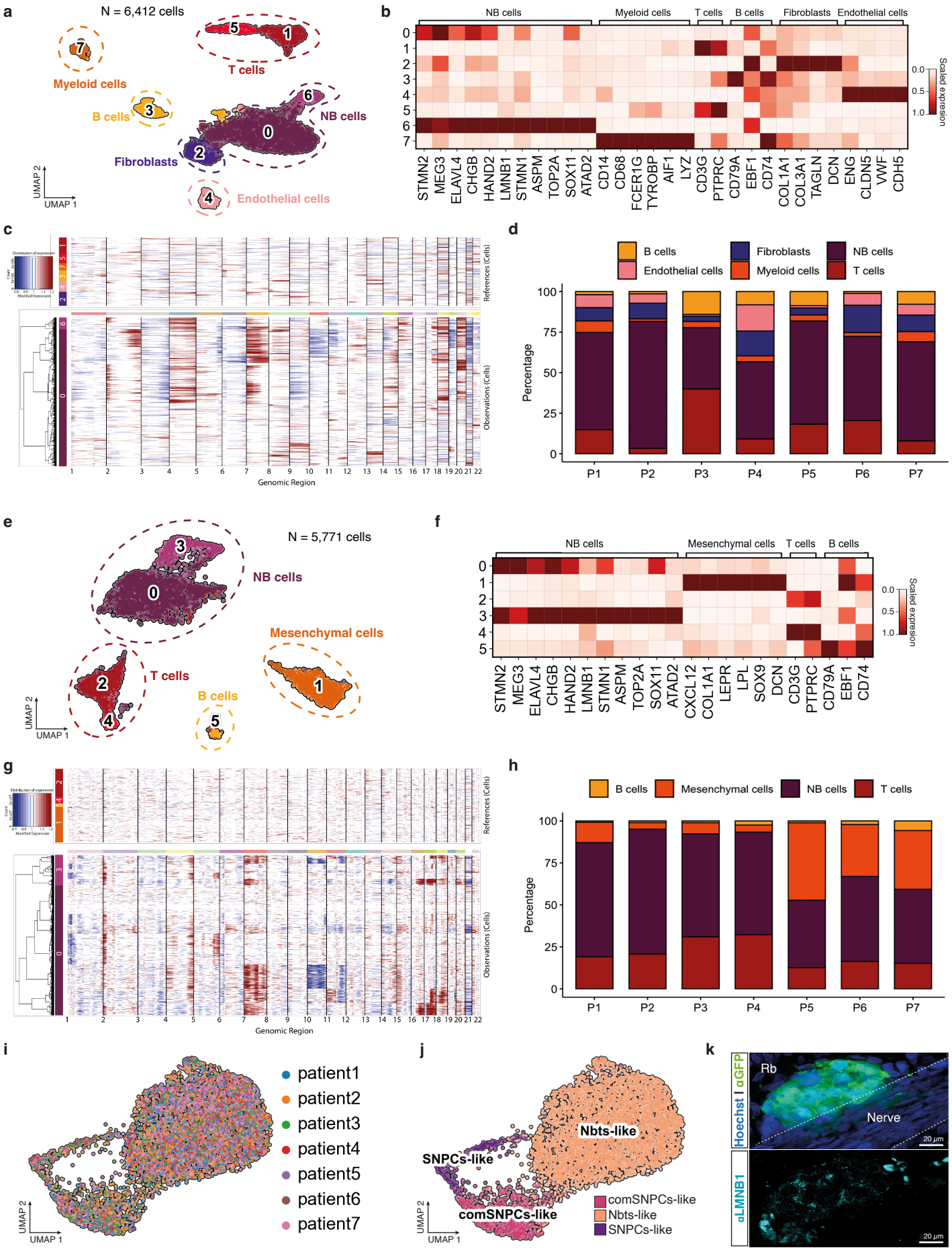

Supplementary Fig. 7 | scRNA-seq data from patient paired primary tumor and invaded bone marrow samples. a, 6,412 cells from 7 NB primary tumor samples integrated in a unique UMAP colored by unsupervised clustering. **b,** Heatmap scaled expression values of marker genes for cell types present in primary tumors. **c,** Inferred copy number profiles of NB cells using InferCNV with non-NB cells as a reference. **d,** Bar plot with fractions of cell types per patient primary tumor sample. **e,** 5,771 cells from 7 invaded bone marrow samples integrated in a unique UMAP colored by unsupervised clustering. **f,** Heatmap of scaled expression values of marker genes for cell types residing in NB-invaded bone marrow. **g,** Inferred copy number profiles of NB cells using InferCNV with non-NB cells as a reference. **h,** Bar plot showing fractions of cell types per patient bone marrow sample. **i,j,** UMAP plot of 6,693 NB cells sub-sampled from 7 integrated paired PT/BM patient samples colored by patient (**i**) and by SA lineage-related transcriptional states (**j**). **k,** Representative images of IGR-N91::GFP cells grafted in the avian embryo disseminating along peripheral nerves and showing heterogeneous expression of LMNB1 identified as a marker of the c2 cluster (observed in N=3/3 embryos from 2 independent experiments). Tissue sections were labeled with α-GFP (green, IGR-N91::GFP cells) and α-LMNB1 (cyan) antibodies. Scale bars are indicated on the photos. Source data are provided as a source data file. *Rb: Rib.*

Supplementary Fig. 8

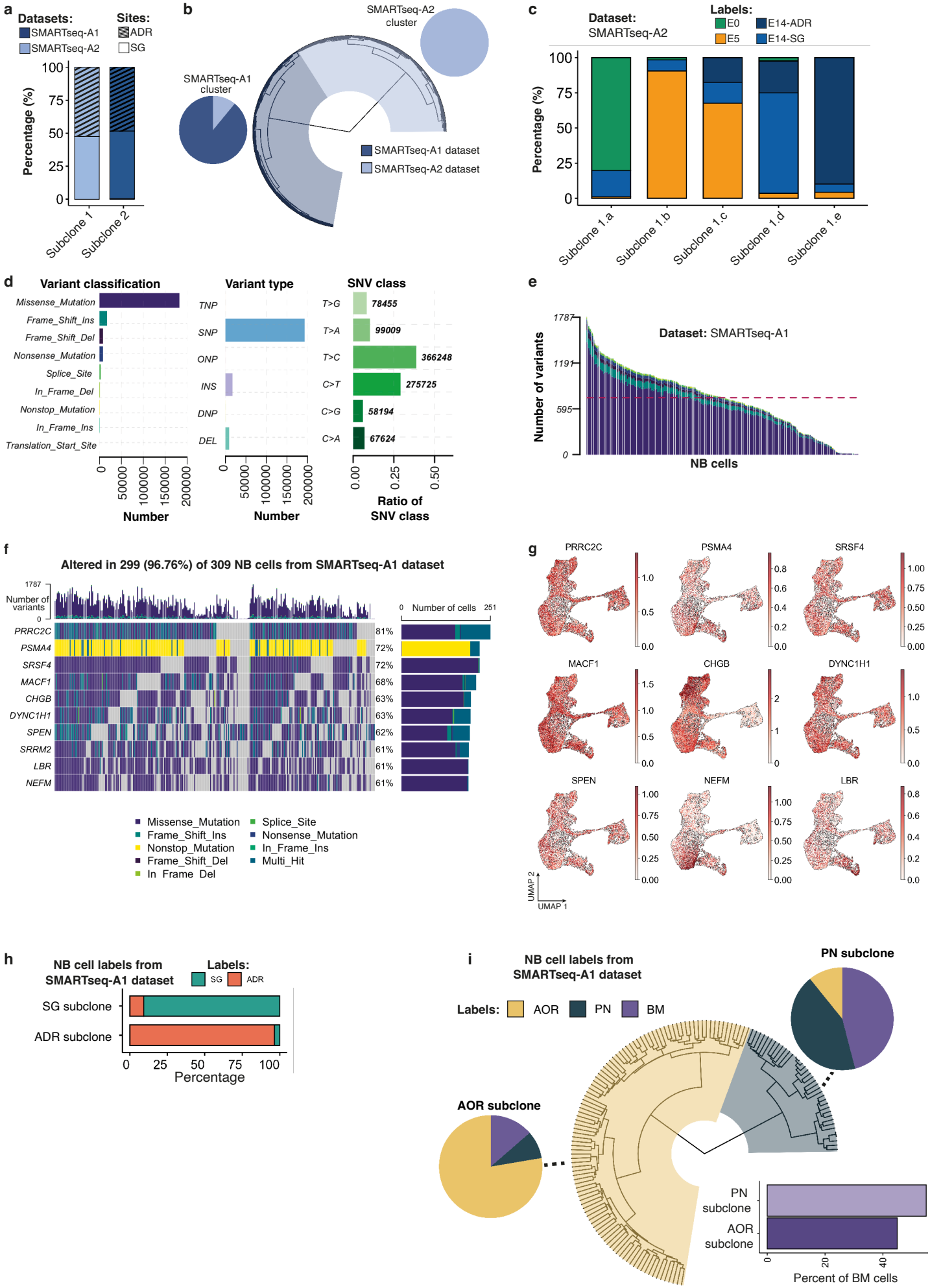

Supplementary Fig. 8 | Single nucleotide alterations extracted from scRNA-seq transcriptomic data of NB cells across metastatic progression in the avian embryo. a,b Bar plot (**a**) and parsimony tree (**b**) showing fractions of IGR-N91::GFP cells harvested from ADR and SG primary tumor sites in E14 embryos, colored by dataset (SMARTseq-A1, SMARTseq-A2), and clustered by genomic proximity of subclones. Genetic proximity between cells was computed using single nucleotide polymorphisms and indel alterations of transcriptomic regions to build a cell-to-cell genetic divergence matrix based on variant allele frequency. **c**, Bar plot showing fractions of IGR-N91::GFP cells, colored by condition over time and anatomical location (included in SMARTseq-A2 dataset: E0 cells in culture; E5: primary SA tumors; E14: primary tumors in SG and in ADR), and clustered by genomic proximity. Genetic proximity between cells was computed as explained in **a**. **d**, Mutation Annotation Format (MAF) summary plot showing bar plots of variant classification (left), variant types (middle; TNP: Triple Nucleotide Polymorphism, SNP: Single Nucleotide Polymorphism, ONP: Oligo-Nucleotide Polymorphism, INS: Insertion, DNP: Double Nucleotide Polymorphism, DEL: Deletion)**,** and class of single nucleotide variations (SNV) (right). **e**, Number of variants per single cell. **f,** Onco-plot illustrating the top 10 mutated genes sorted and ordered by frequency (included in SMARTseq-A1 dataset at E14: SG; ADR; PN; AOR; BM). **g,** Expression of the most frequently mutated genes in UMAP embedding of the human SA lineage. Color scales indicate log-normalized gene expression. **h,** Bar plot showing fractions of cells from primary tumors only (sympathetic tumors, adrenal tumors) clustered by genomic proximity with SG or ADR subclone. **i,** Parsimony tree showing genetic relationships between cells located in the aorta (AOR), on peripheral nerves (PN) and in the bone marrow (BM). AOR and PN cells segregate into two arms (respectively in yellow and in grey) which both comprise BM cells. Genetic proximity between cells was computed as explained in **a-b**, with data extracted from SMARTseq-A1. Below the parsimony tree, a bar plot shows the fractions of cells located in the BM that clusterize by genomic proximity either with AOR subclone or with PN subclone.

Supplementary Fig. 9

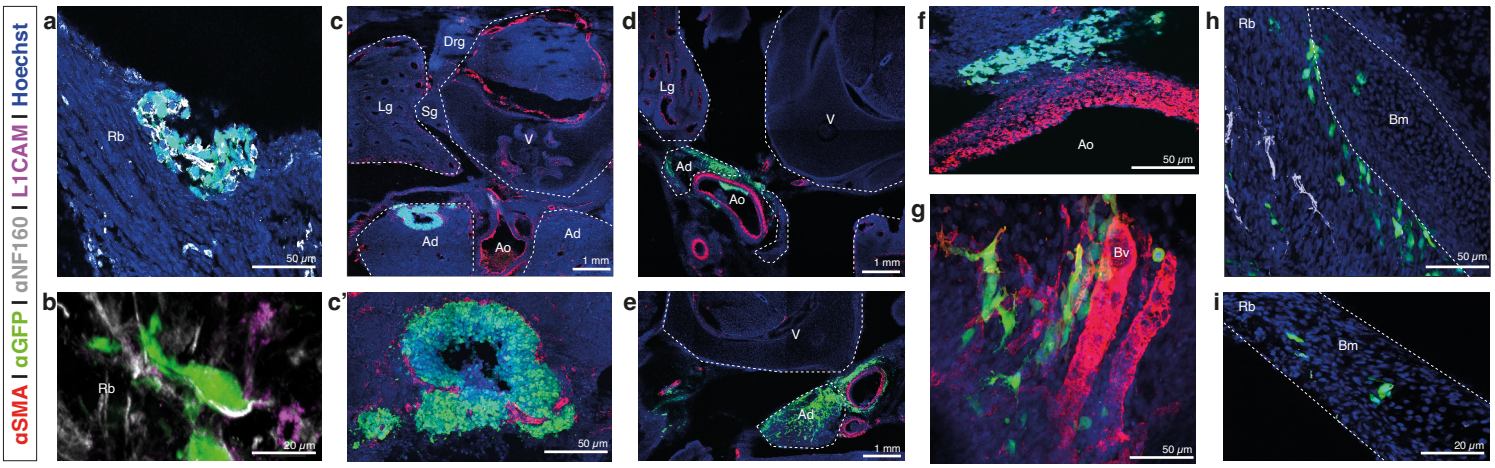

Supplementary Fig. 9 I Analysis of NB dissemination paths by confocal microscopy. Representative images of immunofluorescent labeling using α-NF160 (grey, nervous tracts) or α-SMA (red, blood vessels), α-L1CAM (magenta, nervous tracts) and α-GFP (green, IGR-N91::GFP cells) antibodies on cryosections of E14 chick embryos grafted with IGR-N91::GFP cells. **a,b**, illustrate nerve-associated migration reaching the ribs (rb). **c** (enlargement in **c'**) shows a vascularized adrenal tumor (**c'**). **d-f**, illustrate NB cells transiting from adrenal tumors to the dorsal aorta. **g**, shows NB cells migrating along blood vessels at distance from the primary site. **h,i**, illustrate NB cells in the bone and bone marrow of ribs. For L1CAM immunolabeling, the image was representative of 2 independent experiments. All other images shown were representative of 5 independent experiments. Source data are provided as a source data file. Scale bars are indicated on the photos.
Ad: Adrenal gland; Ao: Aorta; Bm: Bone marrow; Drg: Dorsal root ganglia; Lg: Lung; Rb: Rib; Sg: Sympathetic ganglia; V: Vertebrae.

Supplementary Fig. 10

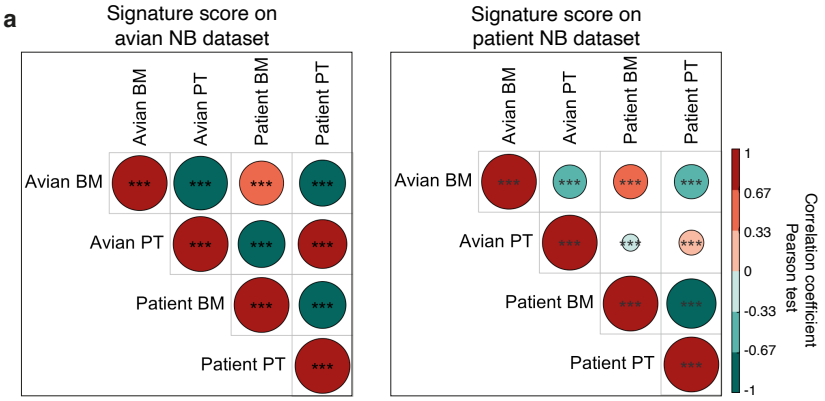

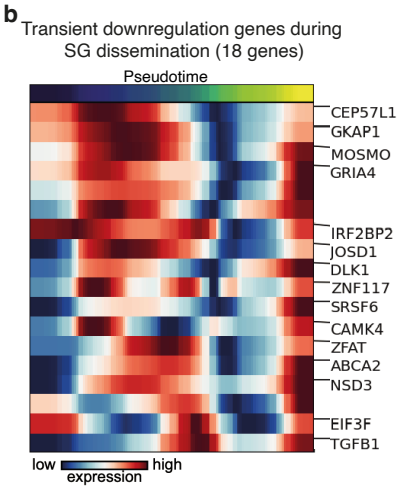

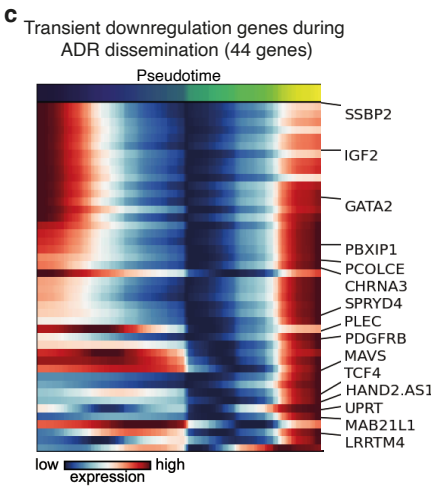

d

	D. 23%	D. 77%
ATP6AP1	-1.25	-0.83
ATP6V0A1	-0.18	0.04
CDK5RAP2	-0.32	-0.08
CDS2	-0.72	-0.30
CELF1	-0.30	-0.07
CNN3	0.03	0.25
EIF4ENIF1	-0.19	-0.07
FBXO31	-0.02	0.14
FHL1	0.14	0.23
FOXK1	-0.36	-0.15
GNAO1	-0.42	-0.14
GSE1	-0.26	0.04
HERC1	-0.03	0.10
ING5	-0.07	0.12
INTS11	-2.20	-1.79
IST1	-0.32	-0.15
IVD	-0.06	0.15
KANSL1	-0.94	-0.74
KCNQ2	-0.05	0.08
KLC1	-0.05	0.14
LONP2	0.05	0.19
LSS	-0.32	-0.09
LUC7L3	-2.14	-1.59
MAU2	-0.73	-0.33
MDK	-0.22	-0.05
MFN2	-0.58	-0.17
MFSD11	-0.45	-0.15

	D. 23%	D. 77%
MYT1	-0.37	-0.04
NCAM2	0.00	0.13
NEK9	-0.08	0.04
NFYC	-0.94	-0.73
NGLY1	-0.33	-0.05
NUMA1	-0.87	-0.54
NUMBL	-0.14	0.05
PCBP2	-1.30	-0.96
PPDPF	-0.02	0.13
PREPL	-0.25	-0.09
RAB5B	0.01	0.15
RABGAP1	0.01	0.14
RBFOX2	-0.17	0.07
RBMS1	-0.13	0.02
RERE	-0.10	0.01
SERINC5	-0.07	0.06
SEZ6L2	-0.01	0.11
SIPA1L3	-0.10	0.03
SLC2A4RG	-0.13	0.07
SLC38A10	-0.24	-0.09
SLC44A1	-0.02	0.09
SMARCC2	-0.21	-0.07
SPAG9	-0.34	-0.16
SPEG	-0.02	0.10
SZT2	-0.17	0.03
TNRC18	-0.05	0.15
TRIM2	-0.02	0.12

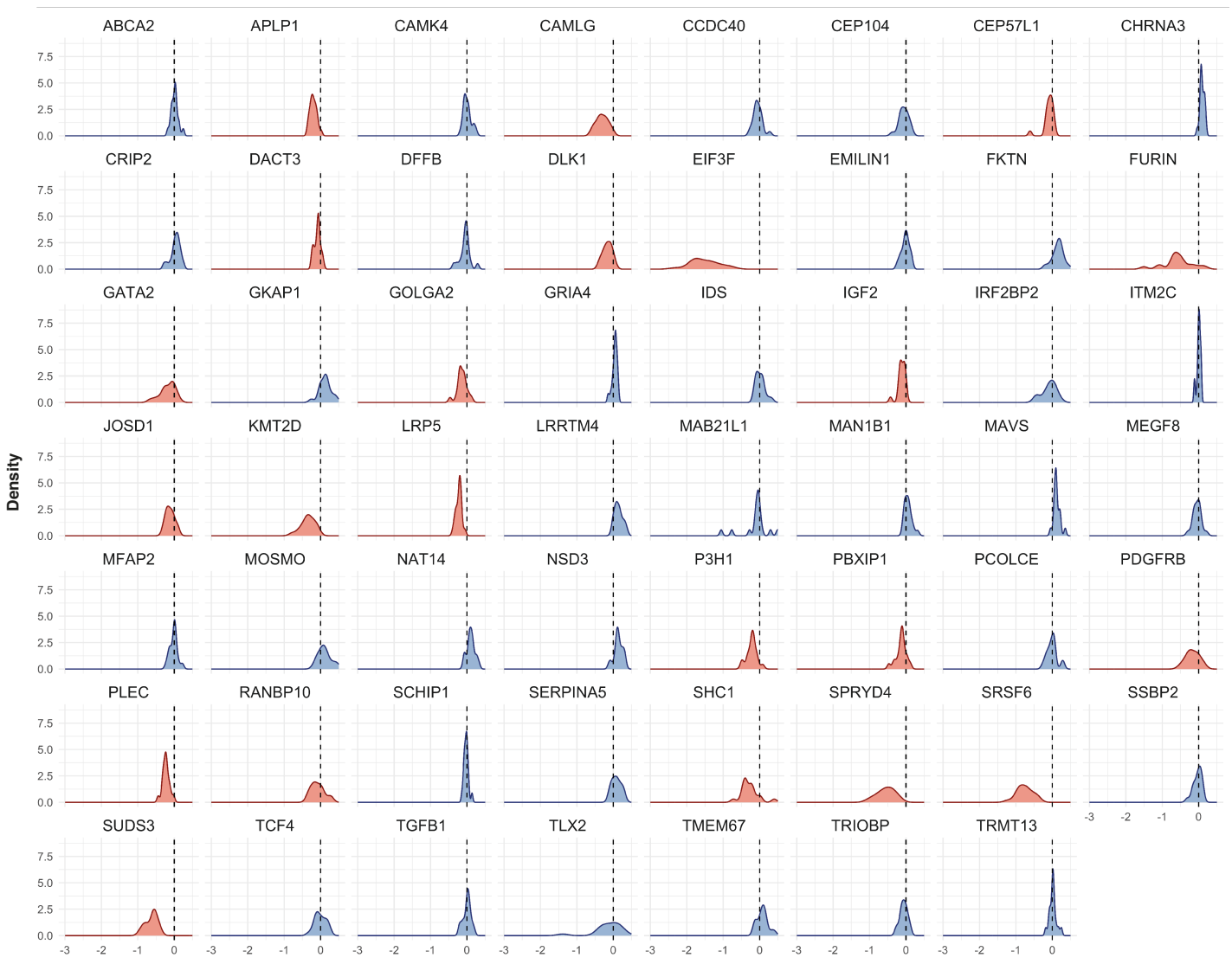

Supplementary Fig. 10 l Analysis of NB BM-genes dependency for cell growth. **a,** Correlative analysis of the expression score of avian-PT, avian-BM, patient-PT and patient-BM gene signatures in NB avian and in NB patient datasets (Pearson test). **b, c,** Set of genes showing transient downregulation during dissemination in the avian embryo from either SG tumors (b, 18 genes) or ADR tumors (c, 44 genes) along linear pseudotime of NB cell trajectories using Moran's I test. **d,e** Distribution of effect scores of the 65 BM-genes (**d**) and of the 62 genes predicted to be transiently downregulated during NB dissemination (**e**) calculated using Chronos algorithms on CRISPR/Cas9 data from DepMap portal on 18 NB cell lines obtained from metastatic sites. The table in **d** shows the dispersion (D) between 23% and 77%. If 77% of the distribution is below 0, the gene is considered to have an impact on cell growth and inversely for a distribution greater than 0. Data are normalized using annotated sets of common-essential and non-essential genes. No effect on cell growth has a score of 0, and a negative score (in red in **d** and **e**) is indicative of gene dependency for cell growth. Source data are provided as a source data file.

Supplementary Table 1. Patient neuroblastoma samples from published data

Dataset	Donor ID	Tissue type	Localization	Age	Sex	Time point	Clinical subtype	State	INSS	Sequencing
Jansky et al. (2021)	NB01	neuroblastoma	intraspinal	< 18 months	M	primary	MYCN	unknown	unkown	Single Cell 3' v2
Jansky et al. (2021)	NB02	neuroblastoma	abdomen	> 18 months	M	primary after chemo	MYCN	unknown	unkown	Single Cell 3' v2
Jansky et al. (2021)	NB03	neuroblastoma	thorax/abdomen	> 18 months	F	primary	TERT	unknown	unkown	Single Cell 3' v2
Jansky et al. (2021)	NB04	neuroblastoma	unknown	> 18 months	F	primary	LR	unknown	unkown	Single Cell 3' v2
Jansky et al. (2021)	NB05	neuroblastoma	cervical lymphnode	> 18 months	F	relapse/metastasis	ALT	unknown	IV	Single Cell 3' v2
Jansky et al. (2021)	NB06	neuroblastoma	adrenal gland	> 18 months	F	primary	LR	unknown	unkown	Single Cell 3' v3.1
Jansky et al. (2021)	NB07	neuroblastoma	pelvis	< 18 months	M	primary	LR	unknown	unkown	Single Cell 3' v3.1
Jansky et al. (2021)	NB08	neuroblastoma	adrenal gland	> 18 months	F	primary	MYCN	unknown	unkown	Single Cell 3' v3.1
Jansky et al. (2021)	NB09	neuroblastoma	throat/neck	< 18 months	M	primary	LR	unknown	unkown	Single Cell 3' v3.1
Jansky et al. (2021)	NB10	neuroblastoma	thorax/abdomen	> 18 months	F	primary	TERT	unknown	unkown	Single Cell 3' v3.1
Jansky et al. (2021)	NB11	neuroblastoma	adrenal gland	> 18 months	M	primary	MYCN	unknown	unkown	Single Cell 3' v3.1
Jansky et al. (2021)	NB12	neuroblastoma	adrenal gland	> 18 months	M	primary	TERT	unknown	unkown	Single Cell 3' v3.1
Jansky et al. (2021)	NB13	neuroblastoma	supraclavicular metastasis	> 18 months	M	relapse/metastasis	TERT	unknown	IV	Single Cell 3' v3.1
Jansky et al. (2021)	NB14	neuroblastoma	occipital subcutaneous bone metastasis	> 18 months	M	relapse/metastasis	MYCN	unknown	IV	Single Cell 3' v3.1
Dong et al. (2020)	T19	ganglioneuroblastoma	adrenal gland	> 18 months	F	unknown	MYCN	Alive	III	Single Cell 3' v3.1
Dong et al. (2020)	T34	neuroblastoma	adrenal gland	> 18 months	F	unknown	non amplified MYCN	Alive	IV	Single Cell 3' v3.1
Dong et al. (2020)	T44	neuroblastoma	adrenal gland	< 18 months	F	unknown	non amplified MYCN	Alive	I	Single Cell 3' v3.1
Dong et al. (2020)	T174	neuroblastoma	adrenal gland	< 18 months	M	unknown	non amplified MYCN	Alive	I	Single Cell 3' v3
Dong et al. (2020)	T40	neuroblastoma	adrenal gland	< 18 months	M	unknown	non amplified MYCN	Alive	IV	Single Cell 3' v2
Dong et al. (2020)	T71	neuroblastoma	adrenal gland	< 18 months	M	unknown	non amplified MYCN	Death	4S	Single Cell 3' v2
Dong et al. (2020)	T27	neuroblastoma	adrenal gland	> 18 months	M	unknown	non amplified MYCN	Death	IV	Single Cell 3' v2
Dong et al. (2020)	T188	neuroblastoma	adrenal gland	< 18 months	M	unknown	non amplified MYCN	Alive	I	Single Cell 3' v3
Dong et al. (2020)	T75	neuroblastoma	adrenal gland	< 18 months	F	unknown	non amplified MYCN	Alive	IV	Single Cell 3' v2
Dong et al. (2020)	T69	neuroblastoma	adrenal gland	> 18 months	M	unknown	non amplified MYCN	Alive	IV	Single Cell 3' v2
Dong et al. (2020)	T200	neuroblastoma	adrenal gland	> 18 months	F	unknown	MYCN	Alive	III	Single Cell 3' v3
Dong et al. (2020)	T92	neuroblastoma	adrenal gland	> 18 months	F	unknown	non amplified MYCN	Alive	IV	Single Cell 3' v2
Dong et al. (2020)	T230	neuroblastoma	adrenal gland	> 18 months	M	unknown	MYCN	Alive	III	Single Cell 3' v3
Dong et al. (2020)	T214	neuroblastoma	adrenal gland	< 18 months	F	unknown	non amplified MYCN	Alive	III	Single Cell 3' v3
Dong et al. (2020)	T10	ganglioneuroblastoma	adrenal gland	> 18 months	M	unknown	non amplified MYCN	Alive	IV	Single Cell 3' v2
Dong et al. (2020)	T162	neuroblastoma	adrenal gland	> 18 months	M	unknown	MYCN	Alive	IV	Single Cell 3' v3
Kildisiute et al. (2021)	NB125	neuroblastoma	unknown	unknown	NA	Pre-treatment	MYCN	unknown	III	Single Cell 3' v2/v3
Kildisiute et al. (2021)	PD43255	neuroblastoma	unknown	unknown	NA	Pre-treatment	non amplified MYCN	unknown	IV	Single Cell 3' v2/v3
Kildisiute et al. (2021)	PD46693	neuroblastoma	unknown	unknown	NA	Pre-treatment	non amplified MYCN	unknown	III	Single Cell 3' v2/v3
Kildisiute et al. (2021)	000CGH	neuroblastoma	unknown	unknown	NA	Pretreated (resection primary)	MYCN	unknown	IV	Single Cell 3' v2/v3

Supplementary Table 2. Patient neuroblastoma samples used for scRNASeq sequecing in this study

Dataset	Donor ID	Tissue type	Localization	Sex	Age	Time point	Clinical subtype	State	INSS	Sequencing	Bone marrow infiltration at diagnosis
This paper	P1	neuroblastoma	adrenal gland	F	> 18 months	Pre-treatment	non amplified MYCN	Alive	IV	CEL-Seq2	
This paper	P1	neuroblastoma	bone marrow	F	> 18 months	Pre-treatment	non amplified MYCN	Alive	IV	CEL-Seq2	0,90%
This paper	P2	neuroblastoma	adrenal gland	M	> 18 months	Pre-treatment	MYCN	Alive	IV	CEL-Seq2	
This paper	P2	neuroblastoma	bone marrow	M	> 18 months	Pre-treatment	MYCN	Alive	IV	CEL-Seq2	1%
This paper	P3	neuroblastoma	adrenal gland	F	< 18 months	Pre-treatment	MYCN	Death	IV	CEL-Seq2	
This paper	P3	neuroblastoma	bone marrow	F	< 18 months	Pre-treatment	MYCN	Death	IV	CEL-Seq2	58,00%
This paper	P4	neuroblastoma	cervical tumor	F	> 18 months	Pre-treatment	non amplified MYCN	Alive	IV	CEL-Seq2	
This paper	P4	neuroblastoma	bone marrow	F	> 18 months	Pre-treatment	non amplified MYCN	Alive	IV	CEL-Seq2	70% / 21.8% *
This paper	P5	neuroblastoma	adrenal gland	F	< 18 months	Pre-treatment	non amplified MYCN	Death	IV	CEL-Seq2	
This paper	P5	neuroblastoma	bone marrow	F	< 18 months	Pre-treatment	non amplified MYCN	Death	IV	CEL-Seq2	2,30%
This paper	P6	neuroblastoma	adrenal gland	F	> 18 months	Pre-treatment	7-8 copies of chr 2	Alive	IV	CEL-Seq2	
This paper	P6	neuroblastoma	bone marrow	F	> 18 months	Pre-treatment	7-8 copies of chr 2	Alive	IV	CEL-Seq2	7,40%
This paper	P7	neuroblastoma	cervical tumor	F	> 18 months	Pre-treatment	non amplified MYCN	Alive	IV	CEL-Seq2	
This paper	P7	neuroblastoma	bone marrow	F	> 18 months	Pre-treatment	non amplified MYCN	Alive	IV	CEL-Seq2	0,40%

* 70% at the left side and 21.8% at the right side of the pelvis that were punctured for this biopsy.